Taylor & Francis
Taylor & Francis Group

Materials Technology
Advanced Performance Materials

ISSN: 1066-7857 (Print) 1753-5557 (Online) Journal homepage: http://www.tandfonline.com/loi/ymte20

Quantitative architectural description of tissue engineering scaffolds

J. C. Ashworth, S. M. Best & R. E. Cameron

To cite this article: J. C. Ashworth, S. M. Best & R. E. Cameron (2014) Quantitative architectural description of tissue engineering scaffolds, Materials Technology, 29:5, 281-295, DOI: 10.1179/1753555714Y.0000000159

To link to this article: https://doi.org/10.1179/1753555714Y.0000000159

Published online: 26 May 2014.

Quantitative architectural description of tissue engineering scaffolds

J. C. Ashworth*, S. M. Best and R. E. Cameron

Arguably one of the most specialised subtopics in porous materials research is that of tissue engineering scaffolds. The porous architecture of these scaffolds is a key variable in determining biological response. However, techniques for characterising these materials tend to vary widely in the literature. There is a need for a set of transferable and effective methods for architectural characterisation. In this review, four key areas of importance are addressed. First, the definition and interpretation of pore size are considered in relation to fluid transport properties, by analogy with filtration research. Second, the definition of interconnectivity is discussed using insight obtained from cement and concrete research. Third, the issue of data scalability is addressed by consideration of percolation theory, as implemented for the study of geological materials. Finally, emerging techniques such as confocal and multiphoton microscopy are discussed. These methods allow the three-dimensional observation of pore strut arrangement, as well holding great potential for understanding changes in pore architecture under dynamic conditions.

Keywords: Tissue engineering scaffolds, Porous materials, Characterisation, Pore size, Interconnectivity, Percolation, Microscopy, Micro-CT

Introduction

Tissue engineering is a multidisciplinary field that combines materials science with cell biology and biochemistry in order to resynthesise damaged tissues and organs.[1] In this field, the use of porous scaffolds involves a number of key considerations. Not only must the bulk structure be mechanically stable, but the pore architecture must have an appropriate effect on cell behaviour, as this will determine the characteristics of new tissue produced at a wound site.[2]

The end goal of tissue engineering is to replicate and regenerate the tissues of the body. A recognised criterion for this is that a tissue engineering scaffold should mimic the extracellular matrix (ECM) of the regenerating tissue.[3] In order to draw up a meaningful comparison between a scaffold and the ECM, scaffold characterisation is a necessity. The problem is that different techniques are favoured by different research groups, and even within one technique, many different approaches to architectural analysis can be seen in the literature. There is a growing need for standardisation of methods for the characterisation of tissue engineering scaffolds. This paper aims to approach this goal by the elucidation of the existing methods available, not limited to those for tissue engineering scaffold characterisation, but also for porous materials in general. In the first section, entitled 'Unique case of tissue engineering scaffolds', key characterisation methods used in tissue engineering literature are described and their limitations are identified. In the following section, entitled 'Potential interdisciplinary characterisation methods', comparisons are drawn with other applications of porous materials research, in the search for promising approaches to these limitations. The final section, entitled 'Limitations and future directions' examines the potential of these approaches with respect to the specific constraints of the tissue engineering application.

The unique case of tissue engineering scaffolds

Specific requirements of tissue engineering scaffolds

Since the porous architecture of a tissue engineering scaffold is often so complex, there is a wide variety of possible parameters that may be used for its description. The most important of these parameters in affecting tissue regeneration will now be introduced.

Porosity is one of the simplest parameters that can describe a porous scaffold. This is defined as the fraction of pore space in the structure and is often over 90% in tissue engineering scaffolds.[1,4] Pore space can fall into any of three categories, depending on the nature of its connection to the surface of the structure: open, closed or blind ended (Fig. 1).[5] Whereas cell transport is directly affected only by open porosity, any porosity may influence the transport of oxygen and carbon dioxide, as well as the degradation rate of the scaffold.[5,6] Total porosity will also affect mechanical stability, which is known to affect the likelihood of scar formation.[7] Implicitly related to porosity is the surface area/volume ratio (SAV). This parameter affects the

Department of Materials Science & Metallurgy, University of Cambridge, 27 Charles Babbage Road, Cambridge CB3 0FS, UK

*Corresponding author, email jca35@cam.ac.uk

Received 28 February 2014; accepted 14 April 2014
DOI 10.1179/1753555714Y.0000000159

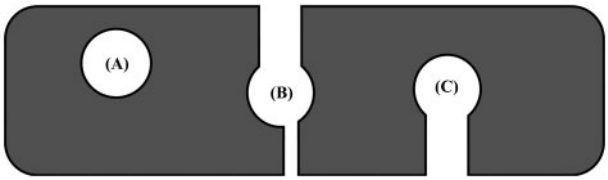

a closed; *b* open; *c* blind

1 Different categories of porosity

ability of cells to attach to scaffold pore walls.[8] Moreover, the scaffold SAV will affect the SAV of the resulting tissue.[9]

Control of pore size in a tissue engineering scaffold is also vital, since subtle changes can lead to significant effects on cell adhesion.[10] Generally, the ideal pore size depends on cell type and should be large enough to allow cell migration through the structure, but small enough to give a high SAV, enabling cells to bind efficiently to the pore walls.[10,11] Pore size is often studied in combination with pore interconnectivity.[12,13] Both can determine the nature of cell movement through a scaffold, for instance whether a cell attaches to one or more walls of a pore,[14] the directionality of cell movement[15] and whether cells move in isolation or as a group.[16]

For cell survivability, a pore network has to be optimised for molecular transport, and this is a function of both interconnectivity and permeability.[17] Permeability describes the ease of fluid flow though the pore space and affects cell nutrition, differentiation and pore accessibility.[18,19] It is therefore capable of influencing tissue formation, by the diffusion of nutrients, waste products and cytokines through the scaffold.[3,20,21] Permeability is determined by various other parameters including porosity and the arrangement of pore struts.[22] It can also be affected by scaffold anisotropy. Any anisotropy in the properties of the desired tissue must also be replicated in the pore structure in order to ensure appropriate tissue regrowth.[23] Anisotropy is also able to affect the migration, shape and alignment of cells.[8,14,24]

It should be noted that changing one property in isolation is often difficult. For instance, variation of pore size is likely also to have effects on the total porosity and SAV, while changing scaffold anisotropy may also affect pore size.[24] The way in which such architectural parameters are related to each other is closely linked to the fabrication technique, and as such, the various techniques commonly used for the fabrication of tissue engineering scaffolds should be briefly studied.

Fabrication: relationship to structure

Broadly, tissue engineering scaffolds are created by one of four processing methods: solvent casting, fibre networking, phase separation and solid free form fabrication. The characteristics of scaffolds formed by each of these processes are summarised in Table 1.

Fabrication routes for tissue engineering scaffolds are closely related to the choice of material. There are three main classes of material that may be chosen.[15] First, natural polymers, such as collagen and chitosan, are typically chosen due to their similarity with the ECM, although they may have poor mechanical properties in scaffold form.[25,26] These materials are heat sensitive, so freeze drying is most commonly used to produce porosity, although electrospinning is also possible.[27] Second, synthetic polymers, such as copolymers of poly(glycolic acid) and poly(lactic acid), are also popular as they may be tuned compositionally to give a wide range of properties, with high predictability.[28] These are often thermoplastics, so they can be processed by a wide variety of techniques, commonly by solid free form fabrication.[18] Finally, bioceramics, such as hydroxyapatite and tricalcium phosphate, may also be used due to their similarity to bone mineral.[15] These are commonly incorporated as additives into polymeric scaffolds, since a pure ceramic scaffold suffers from low toughness.[28] Techniques can also be used to produce pure ceramic scaffolds, such as freeze drying, but this requires the use of sintering as a post-processing step. This leads to additional porosity within the scaffold walls, on a smaller scale to the scaffold macroporosity.[29]

A combination of fabrication techniques may be desirable, since each is particularly suited to a given range of porosity and pore size. Characterisation methods should therefore be chosen to ensure efficacy at the appropriate length scales for the fabrication

Table 1 Summary of most common methods for tissue engineering scaffold fabrication: for more in depth review into such techniques, refer to Ref. 28

Method	Origin of porosity	Key architectural characteristics	References
Solvent casting	Precursor is a solution (or melt). Porogen leaching produces porosity. Shape, size and concentration of porogen controls porosity and pore size.	Pore sizes roughly 100 μm (can vary by an order of magnitude). Low interconnectivity (unless combined with gas foaming).	30,31
Fibre networking	Fibre bonding or electrospinning produces a fibre network. Control of fibre diameter (by deposition parameters) produces porosity variations.	High SAV and similarity to ECM. Limited control of pore size and scaffold dimensions.	19,27,32
Phase separation/ freeze drying	Demixing of a solution or slurry. Freeze drying involves growth and sublimation of ice crystals from a polymer or ceramic slurry. Pore size and shape are varied by alteration of phase separation conditions.	Very high porosities (90% for polymers, 70% for ceramics). Variable mechanical stability. Pores between 20 and 500 μm. Fairly anisotropic structures.	29,33,34
Solid free form fabrication	Precise scaffold architectures are defined by computer aided design, and created by e.g. layer by layer polymer deposition, laser induced polymerisation or 3D printing of a binder.	High porosity and interconnectivity. Resolution limit of 100 μm.	23,35

techniques used. It is important to realise that two different categories of scaffold may not be suited to characterisation by the same method.[5] The next section will elucidate the various possibilities that may be chosen for scaffold characterisation.

Existing characterisation techniques

As mentioned before, one of the simplest descriptions of a porous material is its porosity. This is also one of the simplest to measure, with techniques including simple measurements of relative density, or the Archimedes method based on liquid displacement.[17,36] Whereas relative density describes the total porosity of a scaffold, the Archimedes method describes the accessible (open and blind) porosity only. Other methods include porosimetry, in which a liquid (commonly mercury) is intruded into a scaffold, whereupon the pressure required to do so may be converted to a porosity measurement. This technique also measures only accessible porosity and, moreover, is limited in resolution: porosity below the micrometre scale may not be detected by this technique.[37] In order to detect porosity on this scale, gas adsorption onto the scaffold surface must be measured.[36] Using this method, volume and pressure measurements of the gas (commonly nitrogen), along with theory such as the Brunauer–Emmett–Teller equation, are used to calculate surface area and porosity on the nanometre scale.[17,38]

Owing to the indirect nature of the technique, some assumptions about scaffold architecture have to be made if pore sizes are to be interpreted from porosimetry data.[17,37] The common assumption of cylindrical pores can lead to unrealistic distributions in pore size measurements, with large errors particularly when ink bottle shaped pores are present.[39] Furthermore, mercury intrusion tends to deform soft samples, which can lead to difficulties if it is used for polymer scaffolds.[40]

An alternative approach, one which allows direct observation of the scaffold architecture during characterisation, is image analysis. Scaffolds are imaged primarily either by optical microscopy or by scanning electron microscopy (SEM). Porosity may be measured by counting the number of image pixels taken up by pore space. This tends to give slightly lower values of porosity compared with density measurements, due to the limit of resolution of image data.[41,42] A line intercept method, in which the number of pore/solid interfaces crossing a line of known length is counted, is often used to measure pore size.[6,43] It must be noted that this provides a measure only of the pore cross-sections seen in a two-dimensional (2D) image. The limitations of image analysis are that the acquisition and processing of images can both be time consuming. Sample preparation is often intense: with dehydration, embedding, sectioning and staining of many slices often required for a representative view of the scaffold.[6,44] Image analysis may also be used to measure pore strut thickness, but scaffold complexity is usually too great to allow measurements of SAV from a 2D image.[17] Some authors also use SEM images for observations of scaffold anisotropy, but these are rarely quantitative.[45,46]

Alternatively, a three-dimensional (3D) set of images may be obtained by a tomographic technique: most commonly X-ray microcomputed tomography (micro-CT) or magnetic resonance imaging (MRI). These techniques can be advantageous because they are non-destructive and involve no sample deformation in preparation, and can be used to measure SAV, pore volume and connectivity parameters.[37,47–49] Magnetic resonance imaging uses the nuclear magnetic resonance signal from a fluid filling the pore space (commonly water) as the source of image contrast.[47,50] It is powerful in that fluid velocity data may also be obtained to gain an impression of the effect of the scaffold architecture on fluid flow.[21] The disadvantage is that the resolution of MRI is low, limited to ~50 um.[47] Micro-CT, with available resolutions of 1 μm and lower, has therefore emerged as a key technique for analysis of tissue engineering scaffolds. This technique is based on X-ray attenuation and is high resolution enough for most tissue engineering applications.

Since tissue engineering scaffolds have such high porosity, pore space is often continuously linked throughout 3D space, and therefore, some method is often used to separate the pore space into discrete volumes. The watershed algorithm is a common method of doing so, and this allows pore volume, sphericity and size of interpore connections to be measured.[13,48] Skeletonisation of the pore voxels, to the minimum that maintain the connectivity of the pore space, allows the number and size of interpore connections to be measured.[49] Path lengths and tortuosity (ratio of path length/end to end distance) may also be investigated.[51] Interconnectivity of the pore space is sometimes analysed using erode and dilate functions. These functions, when applied to a tomography dataset, remove or add a layer of pore wall voxels to the pore edges respectively and, when used in combination, have the effect of removing pore features below a certain size, as demonstrated in Fig. 2.[52] This can be an effective method of measuring the sizes of narrow interconnections, as well as their effect on total interconnectivity.[52,53] Figure 3 compares this approach with a similar form of analysis based on a 'shrink wrap' function. This analysis mirrors the process by which cells will invade the pore space, detecting pore accessibility from the scaffold edges given a certain minimum connection size.[54]

Fluid flow techniques may also give measurements of scaffold permeability. The relationship between fluid flow rate through a scaffold and the applied pressure is determined by permeability, as described by Darcy's law.[12] Alternative methods involve calculations based on pore size and geometrical modelling of the scaffold structure,[55] or measurement by spherical indentation tests,[56] but some prior knowledge of the scaffold behaviour is required.

The above serves to provide a summary of the characterisation techniques currently being utilised for tissue engineering scaffolds. However, there are areas of neglect in the interpretation of their results, as well as some scaffold characteristics that are on the whole not sufficiently defined or rigorously measured. The next section will expand upon the most important of these limitations.

Key neglected areas

The first point of note is the discrepancy in the definition of pore size. While many authors favour the linear intercept technique as a means of characterisation,[57] others prefer to measure individual interchannel spacings.[12,58] The example in Fig. 4 demonstrates how these differing approaches can lead to different interpretations

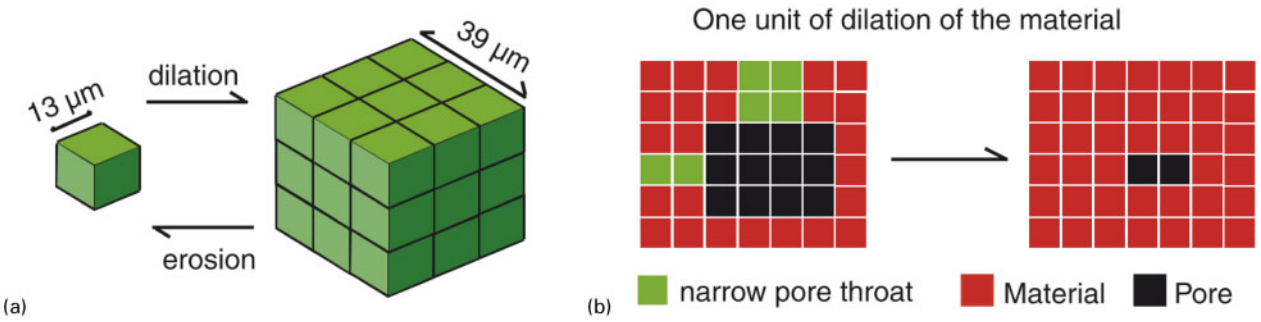

2 Effect of erode and dilate functions on *a* collection of 3D voxels and *b* narrow pore throats: note that carrying out subsequent erosion on end structure in *b* would restore volume of central pore, but not of pore throats (reprinted from Ref. 53 with permission from Elsevier)

of the term 'pore size'. Additionally, some authors place the emphasis instead on interconnecting pore diameters, as measured using physical techniques.[38,59]

Part of the reason for this discrepancy stems from the lack of standardisation in the definition of interconnectivity. This varies considerably from paper to paper, as shown by the range of possible definitions in Table 2. Since interconnectivity is acknowledged to be essential for cellular invasion and nutrient flow,[15] it is worrying that there is no established standard for its measurement. In some cases, a qualitative observation of the interpore connections is made from SEM images; in others, the authors conclude that their scaffolds must be interconnected as a result of observed cellular invasion.[63,64] Attempts at quantitative measurements are equally varied. For instance, Maspero *et al.*[65] used maximum pore/solid distances as a measurement of interconnectivity. Despite measuring these distances as between only 12·5 and 25 μm (compare this with the suggested interconnect sizes of 80 μm given in the literature),[38] the authors conclude that the interconnectivity of the scaffold studied would be sufficient to allow tissue ingrowth and vasculature, with no test of this hypothesis. Another approach by Lin *et al.*[60] involved use of a micro-CT dataset to measure the size of the largest connected pore domain, relative to the total pore space. The issue is that this type of measurement will be dependent on the voxel size of the micro-CT dataset. The approach by Moore *et al.*[52] described in the section on 'Existing characterisation techniques' is a more meaningful alternative, as it describes the proportion of accessible pore space as a function of connection size. This is perhaps the most promising approach of all the different options, although it has an important limitation as will soon be elucidated.

When obtaining 2D or 3D scaffold images, the limited field of view introduces a problem with the scalability of data measured from these images. A simple example would be a 2D image that is smaller than the largest pores in the structure. Clearly, this would lead to an underestimation of pore size in the scaffold as a whole, but is fairly easy to overcome by imaging at more than one magnification. Other scaling problems are more subtle. For instance, an equally valid variation on the measurement technique of Moore *et al.*[52] was used by Lemon *et al.*,[66] to obtain interconnectivity as a function of connection size. However, in this case, there is a potential problem in the data presented. Lemon presents values of interconnectivity, defined as the proportion of accessible pore volume, dropping to values of ~10% for

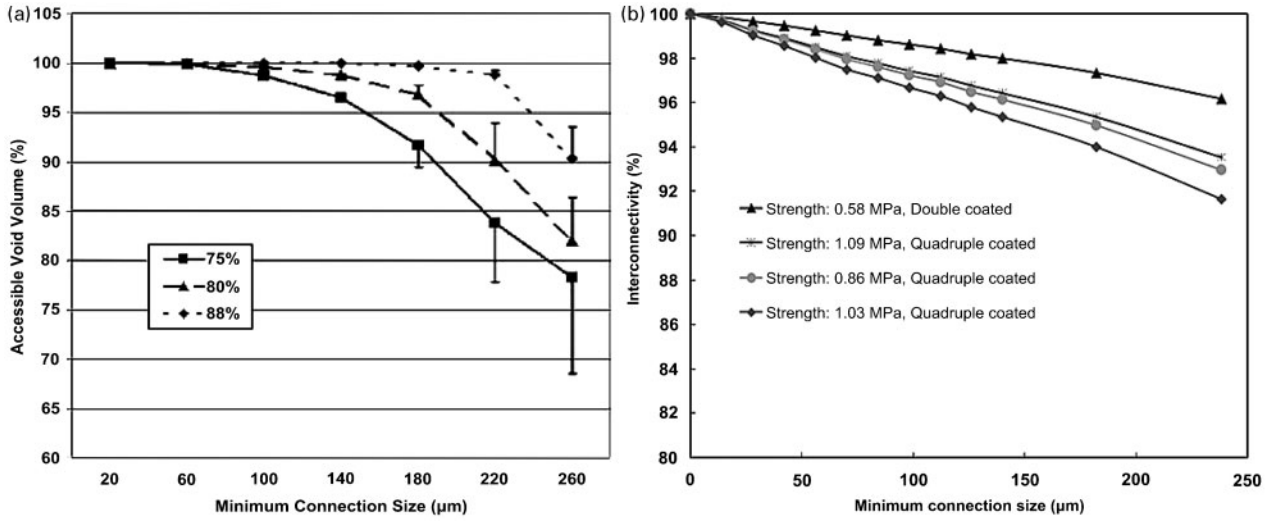

a erode and dilate operations (on polymer scaffold with various porogen fractions as indicated); *b* shrinkwrap function (on ceramic scaffolds with various processing parameters)

3 Comparison of interconnectivity measurements obtained using two different methods (reprinted figures: *a* from Ref. 52 with permission from Wiley and *b* from Ref. 54 with permission from Elsevier)

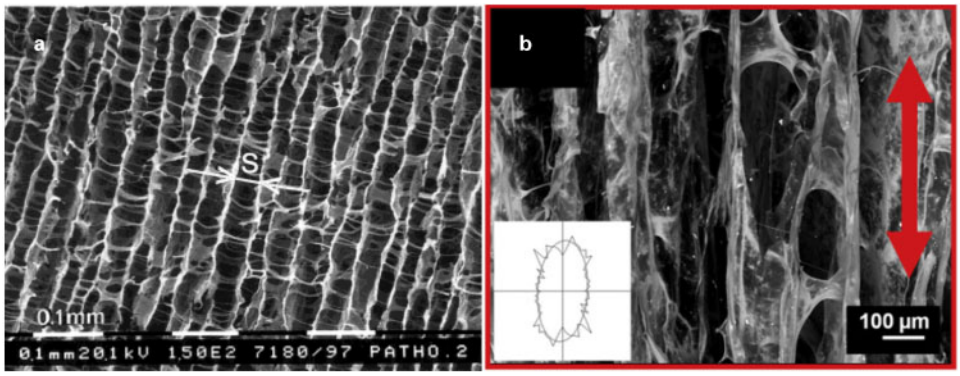

a channel width measurements (S=pore size); *b* linear intercept method to define average pore ellipse

4 Comparison of two different approaches to pore size definition in anisotropic scaffolds (reprinted figures: *a* from Ref. 58 with permission from Wiley and *b* from Ref. 57 with permission from Elsevier)

the largest connection sizes tested (*see* Fig. 5). The issue here is the location of this accessible porosity, which the authors note to be near the scaffold surface. This means that the observed results will be dependent on the total volume of the 3D dataset, since in a larger volume, the surface porosity will make up a smaller proportion of the total porosity. This will therefore lead to different measured values of percentage interconnectivity depending on the size of the scaffold volume analysed. It is vital that data scalability is considered in extrapolating the measurements made on small scale images to properties that may describe the whole scaffold.

The arrangement of the pore struts or walls is a further parameter that must be understood. One way in which pore wall characterisation is well established is in the measurement of pore wall porosity using gas adsorption. However, the effect of an anisotropic arrangement of pore struts on cell behaviour has not yet been adequately characterised. Harley *et al.*[67] have observed the importance of struts and strut junctions in determining the speed of cellular migration through collagen scaffolds. The focus in the literature is, however, on the characteristics of pore space rather than pore walls, and this approach is likely to be an oversimplification.[15]

The main areas of neglect in the characterisation of tissue engineering scaffolds may therefore be summarised by the following four points:

(i) the definition and interpretation of pore size
(ii) the definition of interconnectivity
(iii) data scalability
(iv) measurement of pore strut arrangement.

Tissue engineering is far from the only research field that makes use of porous materials. Any field that makes use of such materials must have associated characterisation techniques for materials optimisation. Therefore, it may be that suitable approaches to addressing these key issues lie in other areas of porous materials research. As such, a discussion of the most likely scaffold characterisation techniques from such related areas will now follow.

Potential interdisciplinary characterisation methods

Porous materials in other research fields

First, it may be useful to examine how biological scaffolds fit into the broader picture of porous materials research. Figure 6 shows a representation of the various different categories of porous material. As can be seen, these materials are used in a variety of applications, from porous catalysts to load bearing components.

As well as according to the proportion of open porosity, these different porous media may be classified as either structural or functional (*see* also Fig. 7).[100,101] Structural foams often contain closed pores, as openings within the pore walls can act as mechanical defects.[68] In functional porous materials, the pore surfaces and pore accessibility are most relevant.[69] By classifying tissue engineering scaffolds according to this functional–structural scale, it may be seen which research fields could contain the most appropriate characterisation techniques in relation to tissue engineering. It may be seen from Fig. 6 that biomedical implants were originally categorised as structural materials rather than functional. This suggests a material that is designed to be inert in response to the body. However, modern use of the term 'biomedical materials' actually refers to materials that elicit a more active response from the body.[70] Mechanical stability is still required, but this is often true of a porous material whether or not the primary function is structural.[71] It seems that tissue engineering scaffolds fit most closely into the open pore, functional end of the porous material spectrum, and as

Table 2 Selection of interconnectivity definitions from literature

Interconnectivity definition	Author
'The number of pore crossings per unit length along a skeletonised pore backbone'	ASTM[5]
'Extent of a pore connected with its neighbours'	Li *et al.* 2003[12]
'Tortuosity'	ASTM[37]
'Void space remaining accessible to outside air at increasing minimum connection sizes'	Moore *et al.*[52]
'The number and size of connected pore space domains'	Lin *et al.*[60]
'Pore volume inaccessible for a virtual object of varying sizes'	Hacker *et al.*[61]
'Diameter of the opening between adjacent pores'	Mehdizade *et al.*[62]

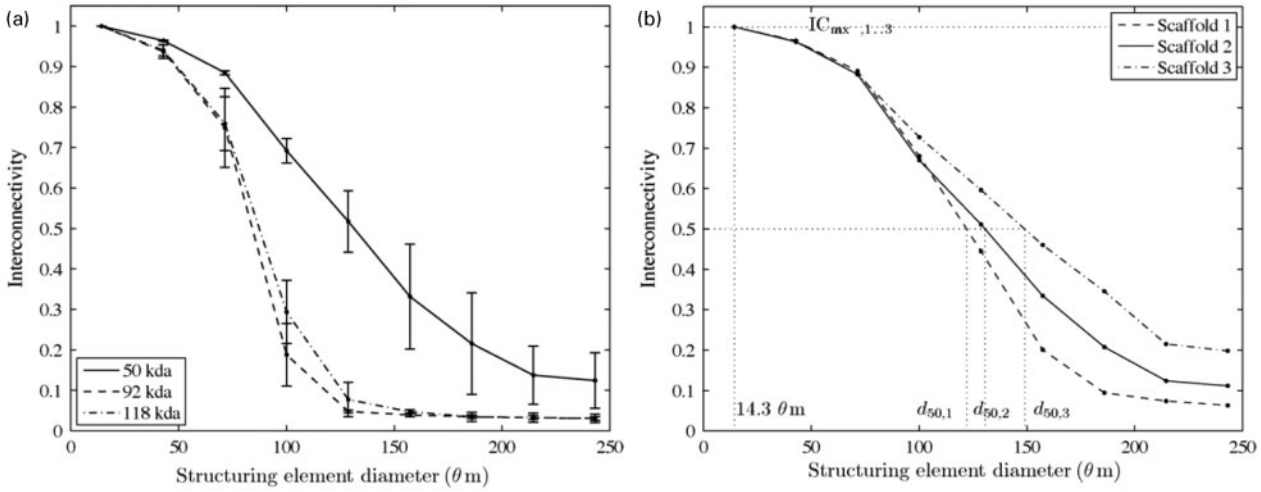

a for comparison of scaffolds made from different molecular weights of PLGA; *b* for definition of two numerical interconnectivity parameters (IC_{max} and d_{50})

5 Graph showing method of Moore *et al.*[52] applied to low interconnectivity scaffolds: note low interconnectivity values in comparison with those displayed in Fig. 3 (reprinted from Ref. 66 with permission from Elsevier)

such, other materials of this description are the most appropriate comparisons.

Potentially transferable techniques

Three key areas of porous materials research have been identified that may hold promise for enhancing the characterisation potential of tissue engineering scaffolds: filtration research, cement and concrete, and porous rocks as studied by geoscience. These areas are all characterised by a focus on characterising porous architecture with reference to the overall connectivity properties of the structure.

Filtration: pore size

The connectivity of the pore space often leads to difficulties in definition of discrete pore volumes. Filtration research contains two possible solutions to this difficulty. The first of these, developed by Lin *et al.*,[72] uses a micro-CT dataset to measure pore size as a function of connection size. This is based on the same erode and dilate functions as shown in Fig. 2: their successive use is able to break narrow pore connections. If two initially connected pores are separated after a dilation and successive erosion, then the average volume per pore will decrease, while the total number of pores increases. Since the number of dilation and erosion steps used will determine the minimum interpore connection size, a pore size histogram will change depending on the number of erode and dilate operations carried out. This is particularly important for tissue engineering, as it may provide a method for examining the effective pore size distribution as a function of the size of the cell inhabiting the scaffold. Figure 8 shows a typical pore size histogram after such an operation. The histogram is truncated at 100 μm, indicating that this is the pore size distribution that would be encountered by an invading object of 100 μm in size.

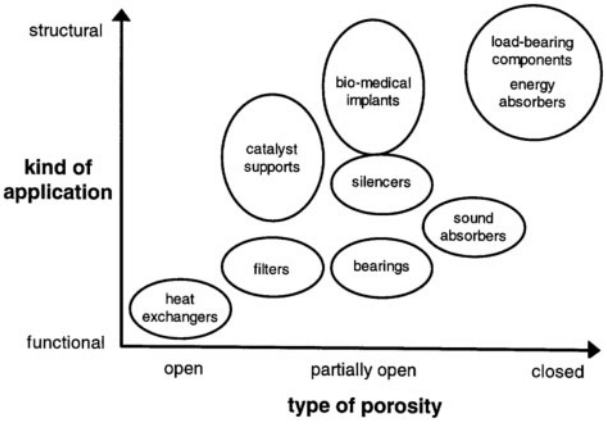

6 Different classifications of porous materials (reprinted from Ref. 69 with permission from Elsevier)

The second approach is based on the physical movement of a fluid through the structure. Mercury porosimetry and its limitations have already been mentioned, but there are other possibilities including capillary flow porometry and extrusion porosimetry, for which a wetting liquid is used instead.[39] These techniques are advantageous in that the pore sizes measured represent the physical pore sizes that will be encountered by an infiltrating object (e.g. a cell) in a hydrated scaffold.[17] They are established techniques in filtration research and, furthermore, are capable of making measurements in dynamic situations, as a function of direction through a material and also of permeability.[39] Since capillary flow porometry measures the most constricted part of each pore, while extrusion porosimetry measures the whole range of diameters, their combination may be the best approach to describe scaffold pore distributions most fully.[37] Capillary flow porometry in particular is beginning to be noticed by the tissue engineering community,[73] but the technique is still far from established in this field.

Cement and concrete: interconnectivity

Interconnectivity is a more complex parameter than is currently acknowledged in tissue engineering literature. In relation to cement and concrete research, Levitz[74] defines three levels of complexity in the architectural description of a porous material: the first level describes the whole material (porosity and SAV), the second the pore space (pore shape and size) and the third the topology of the pore/material interface (including

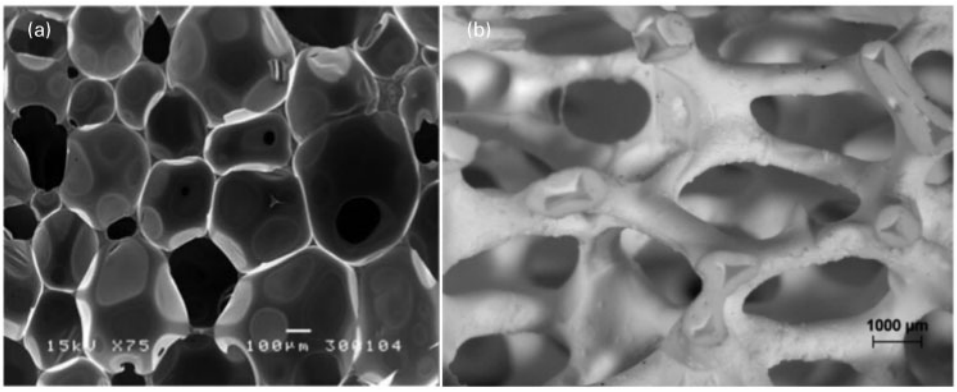

a structural (closed pores); *b* functional (open pores)

7 Examples of porous materials for different applications (figure reprinted with permission: *a* copyright 2010 by Ref. 101 reprinted by permission of SAGE and *b* from Ref. 101 copyright 2009 Americal Chemical Society)

interconnectivity). The topology of the pore/material interface is most readily measured from tomographic datasets. In the study by Promentilla *et al.*,[75] micro-CT is used to produce a list of parameters that may be used to describe this, including some of those listed in Table 2. One such parameter is tortuosity, which can be measured in each of the three dimensions of a scaffold. Crucially, many of these different concepts can be linked to each other by a 'formation factor'.[75] This factor is a description of the dependence of tortuosity on scaffold architecture (*see* Fig. 9) and has also been studied in relation to transport properties in tissue engineering.[76] It can be expressed as tortuosity normalised by porosity, but for many applications, it is more meaningful to normalise by effective porosity.[77] The use of this parameter is promising in that it combines more than one aspect of scaffold interconnectivity, and normalisation by different categories of porosity may provide a comparison between scaffold accessibility to oxygen diffusion, nutrient transport and cell migration.

Porous rock structures: percolation

The above method for interconnectivity requires measurement of effective porosity. This is a key concept in percolation theory, which is a very commonly used approach for studying transport properties in geoscience.[78,79] In a 3D representation of a porous material, there will be continuous groups or 'clusters' of pore space voxels that form pathways through the structure. For a constant structure, the size of the largest cluster will increase with porosity. When a cluster approaches the size of the porous object, so that it is in contact with both surfaces, this cluster is said to be 'percolating'(*see* Fig. 10).[80] In other words, it becomes classified as open porosity rather than blind or closed porosity. Effective porosity should be calculated as the volume of all the percolating pore space clusters normalised by the total scaffold volume.[75]

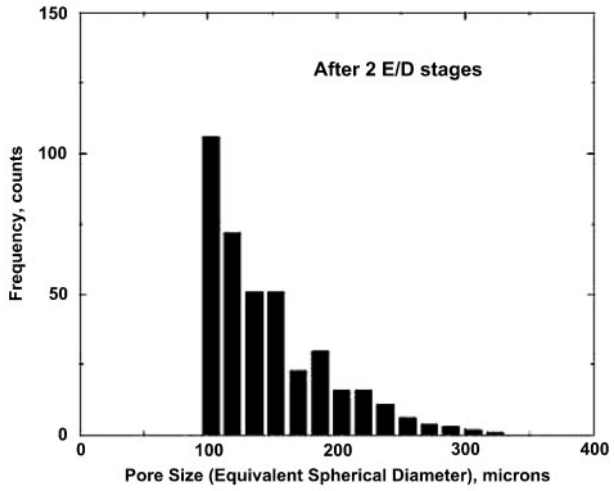

8 Effect of erode and dilate operations (*see* Fig. 2) on pore size histogram (reprinted from Ref. 72 with permission from Elsevier)

This also gives rise to the concept of 'percolation threshold', which is the minimum porosity at which a cluster big enough to connect both sides of a structure exists.[80] The lower the percolation threshold, the more intrinsically connected the structure (a connective cluster exists even when the total porosity is reduced to low values). The value of this percolation threshold may be key in describing the topology of the pore space: since different arrangements of pore space and solid material have been shown to give different percolation thresholds.[81]

To determine the percolation threshold, constant structures of varying porosity are required, in order to determine the minimum porosity to contain a percolating cluster. This may be achieved by applying erode and dilate operations to an existing micro-CT dataset: erosion of a pore wall will increase the porosity but maintain the same structure.[80] This method provides a quantitative measurement of interconnectivity, suitable for comparison and ranking of tissue engineering scaffold structures.[82] However, it is important to consider data scalability. As shown by Sotta and Long,[81] the percolation threshold will change depending on the dimensions of the sample measured. The result of this is that a small scaffold sample may appear to be fully interconnected, but a larger sample may actually have effectively lower interconnectivity. However, percolation theory contains the tools to scale up measured values from small samples and determine their values in bigger samples. The comprehensive paper by Liu *et al.*[80] describes the ways in which micro-CT data may be tested for scalability, with reference to percolation theory. The analysis undertaken includes the calculation of various scaling parameters, as well as percolation threshold, in order to extrapolate characteristics such as permeability from the microscale up to the macroscale. This approach is demonstrated to be effective for widely

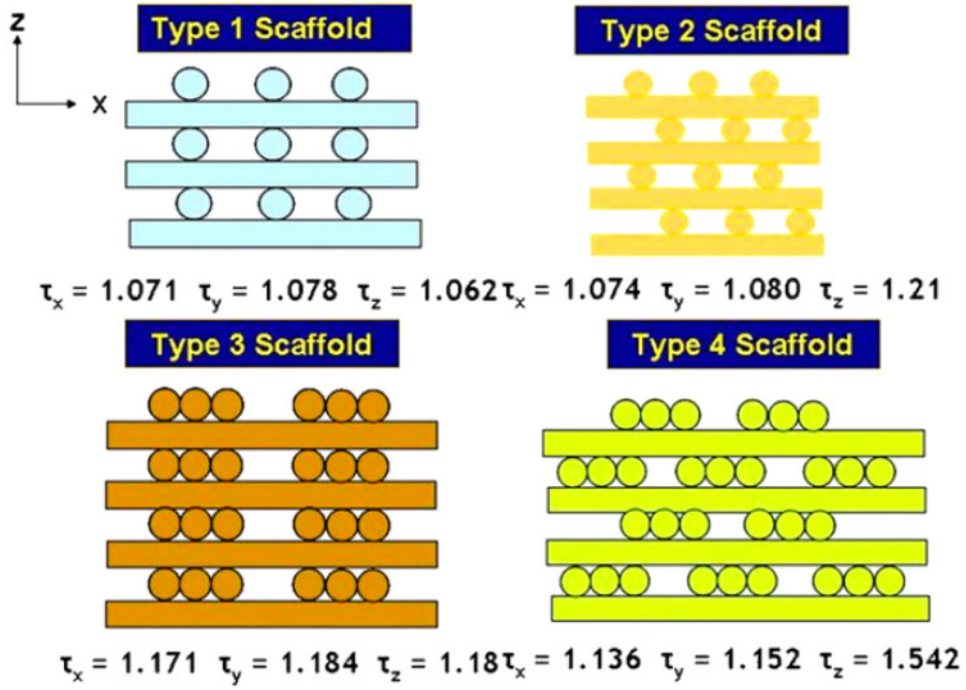

9 Diagram showing how differences in tortuosity (given in each of three dimensions for each scaffold) can arise from differences in scaffold architecture (reprinted from Ref. 76 with permission from Elsevier)

varying classes of porous materials from sandstone to bread.[80]

Percolation may also be examined in different directions.[81,83] This is particularly relevant for anisotropic tissue engineering scaffolds, for instance where pore channels are favoured in order to enhance directional cell invasion. It should be noted that, for soft systems, the percolation threshold should not be considered as a limit, but as a transition between two types of movement e.g. initiation of matrix remodelling by invading cells.[24,84] In combination with directional measurements of tortuosity, however, this approach has promise for providing a rigorous description of the connectivity characteristics of tissue engineering scaffolds.

Benefits and limitations

From the discussion above, it seems that other areas of porous materials research might hold clues to the development of at least some of the key areas identified in the above sections. The potential of these borrowed techniques should now be assessed in terms of their ease of implementation and transferability to tissue engineering research.

Since many of the suggested techniques require the use of a micro-CT dataset, the limitations of micro-CT as a technique must be considered. Although 3D image data can be preferable to 2D images when available, there are several intrinsic limitations to the technique. Porosity is often observed to increase as resolution increases, surface areas are often overestimated and a segmentation process is required to define which pixels/voxels represent pore space, and which represent solid material.[85] The simplest segmentation method is a threshold intensity value, whereas other methods detect edges using texture or brightness as indicators of change.[5] A study by Kline and Ritman[51] compared several methods and observed that measured pore diameter does have a slight dependence on the segmentation method chosen.

However, such segmentation errors are intrinsic to all imaging or tomographic techniques.[86] This means that micro-CT is still a favourable choice when direct image data are required. Therefore, a combination of micro-CT based techniques, and indirect techniques that are more focussed on characteristic lengths relevant to motion through the scaffold (such as capillary flow porometry), might be the best approach to thorough characterisation. In terms of defining pore sizes, both methods described in the section on 'Filtration: pore size' examine pores while simultaneously considering the connectivity of the system. The advantage of this is that there is much less confusion as to which part of the pore is being measured, since the pore size in each case relates to a given application.

In terms of interconnectivity measurements, percolation threshold is a scalable quantity describing the accessibility of scaffold pore space. However, the limitation when compared to techniques such as those by Moore *et al.*[52] and Fostad *et al.*[54] is that it does not describe pore interconnectivity as a function of connection size. Although descriptions of interconnectivity in terms of single voxel pathways are important, they are limited in that they do not indicate how easily a larger object, such as a cell, may invade a structure. A recent paper by Saxton[84] gives some potential insight into this problem. One approach is to consider the excluded volume, or the volume of pore space that cannot be occupied by an object of given size.[87] Figure 11 shows that plotting excluded volume against object size produces a very similar graph to those presented by Lemon *et al.*,[66] with the important difference that the values are scalable. The approach is slightly less intuitive, however, as it does not describe pore accessibility from the outer surfaces of a scaffold. The

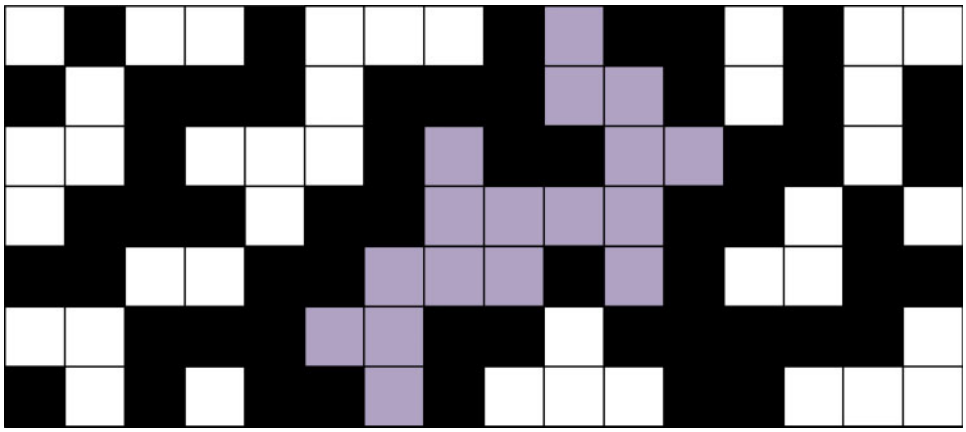

10 Illustration of a percolating pore cluster (shaded, or coloured purple online) in a 2D lattice model. For the lattice dimensions shown, this cluster is large enough to connect top and bottom boundaries, and is therefore percolating. Black lattice sites indicate pore walls, white indicates blind or closed porosity

concept of 'percolation diameter' is therefore introduced. This can be defined as the diameter of the largest particle for which a percolating path through the entire structure exists. Percolation diameter has vast potential for the characterisation of tissue engineering scaffold connectivity, since it has the following key benefits:

(i) it is readily calculable using very similar techniques to Moore *et al.*
(ii) it provides a single value that succinctly describes the connectivity properties of a scaffold
(iii) being based on percolation theory, the quantity is intrinsically scalable.

The one key problem area that remains is the measurement of pore strut arrangement. This is an important parameter in determining the ability of cells to attach to scaffold walls, as well as affecting scaffold permeability.[22] The resolution of a micro-CT dataset is not quite sophisticated enough to allow detailed visualisation of pore struts, and dynamic techniques such as flow porometry are not currently able to make direct measurements of strut arrangement. It is therefore time to turn back to the original application and assess whether the insights gained from other areas of porous materials research are able to guide the future of tissue engineering scaffold characterisation.

Limitations and future directions

Tissue engineering environment

A discussion of the benefits of techniques such as tomography is all very well, but it is important to consider the applicability of measurement techniques in laboratory conditions to the actual behaviour of a scaffold *in vivo*. There are three key considerations to be made here. First, and perhaps most obviously, the pore spaces will not be filled with air, but with cells and biological fluids. This means that the scaffold may well have a different morphology *in vivo* if the structure is strongly dependent on hydration. Second, the acidic conditions, hydration and possibility of proteolytic remodelling by invading cells will lead to eventual degradation of the scaffold.[88] This is a problem in that such parameters as pore size, SAV and porosity can be affected during degradation.[3,89] Finally, since the scaffold will be inhabited by cells, the properties of a

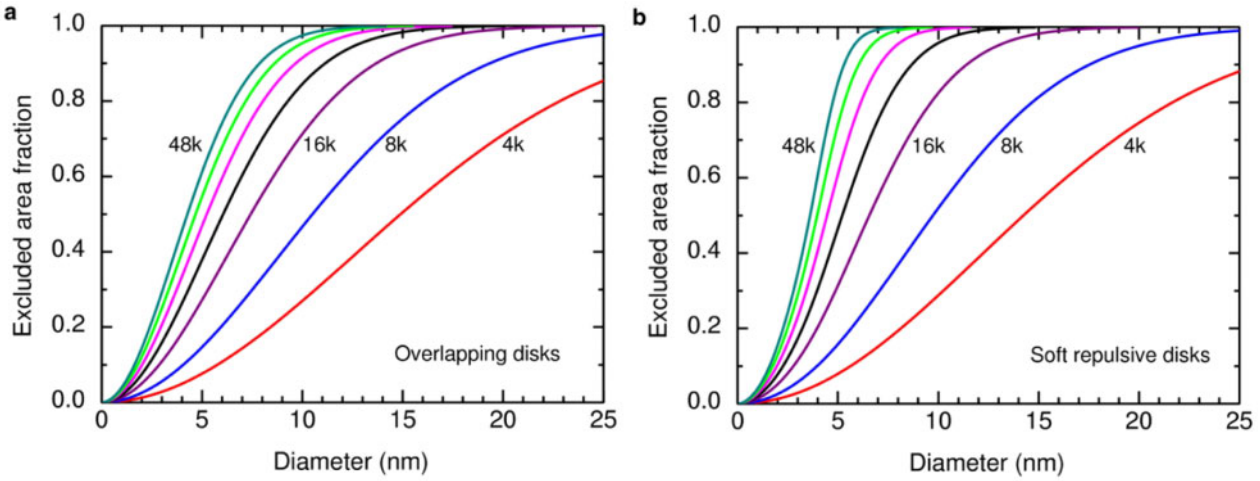

11 Graphs showing relationship between excluded area (equivalent of excluded volume in 3D systems) and diameter of invading object, as calculated using percolation theory: within each graph, different trends indicate different porosities, with each graph indicating different structural configurations (reprinted from Ref. 84 with permission from Elsevier)

scaffold with respect to cell response should be considered. Part of this will be included in the effect of scaffold degradation, but another aspect is the effect of pore struts on cell behaviour in a hydrated scaffold. In addition, cells in a wound site will exert contractile forces on the scaffold material.[90,91] Therefore, the response of scaffold architecture to deformation should also be considered carefully.

Micro-CT is increasingly used for measurements of architecture in response to deformation.[85] The change in morphology during loading, failure mechanisms and strain distributions may be ascertained using this technique.[92] However, while micro-CT can be carried out in the wet state for some materials,[93] there is a limitation in that the X-ray attenuation from water will be very similar to that of natural polymers. The ideal characterisation technique would share the 3D visualisation capacity of micro-CT, but have the additional capability to image hydrated scaffolds, with particular focus on the strut arrangement, and also be able to record the changes in architecture during the processes of degradation and mechanical deformation. Although not yet fully established, techniques do exist in the literature that may eventually allow these considerations to be fully accounted for, and these will now be examined.

Existing solutions

A very simple measurement of the effect of scaffold hydration can be made by studying the swelling behaviour of scaffolds in various physiological fluids.[94,95] From this type of measurement, estimations of the effect of hydration on parameters such as pore size can be made. However, this relies on assumptions such as homogeneous swelling, and so direct observation of the effect of hydration would be preferable. One possible technique to allow this is environmental SEM (ESEM). This technique is very similar to conventional SEM, with the important distinction that wet and insulating samples may be imaged without prior specimen preparation. This is achieved by maintenance of a low pressure gas (often water vapour) around the sample, to provide positive ions by gas electron collisions, compensating for charge build-up on the material surface.[96] This technique has already been used for pore size measurements in tissue engineering scaffolds,[8] but the disadvantage is that it is a 2D technique, so the range of parameters that may be measured is limited.

Another approach might be to combine 2D measurements from ESEM with dynamic measurements of scaffold architecture. For instance, the approach taken by Sell *et al.*[32] involved pore and fibre size measurements of electrospun scaffolds first from image analysis (SEM) and second by calculation from permeability experiments. On comparison of the results from these two techniques, the fibre diameters gave very similar results, indicating the reliability of the permeability measurements. However, pore size measurements were different, indicating that there are differences between the pore dimensions that may be measured from image analysis and the physical pore dimensions that may be encountered in a fluid transport scenario. This further suggests that a combination of physical measurements and image based analysis is needed to characterise a tissue engineering scaffold completely.

There is a remaining problem, which is the lack of a method to measure 3D scaffold architecture in a hydrated or dynamic state. However, there is such a technique, albeit more commonly used for observation of cell behaviour. Confocal microscopy is an optical technique that involves the use of an hourglass shaped beam (illuminating only a small volume of the sample) and a pinhole to select only the required part of the returning beam.[86] In this way, both lateral and vertical resolution can be controlled, and 3D visualisation of a scaffold may be achieved as seen in Fig. 12, by optically sectioning at successive heights.[31] The main limitation is the relatively low z-extent possible, compared with the image dimensions available in the x and y axes.[86]

Bagherzadeh *et al.*[73] provided an advance in this technique, by incorporating commercially available quantum dots as part of the scaffold fabrication process from polymer solution. This allowed more efficient visualisation of the scaffold by confocal microscopy, due to the fluorescence properties of the dots. The 3D dataset obtained was then used to measure pore and interconnect sizes, along with interconnectivity and porosity, by image analysis. As for the approach by Sell *et al.*,[32] these measurements were combined with those from physical pore size measurements, in this case from capillary flow porometry, in order to present a complete view of the scaffold properties.

The advantages of confocal microscopy for examining scaffold architectures are numerous. First, the scaffold may readily be imaged in a hydrated state, allowing the pore and strut arrangements that will exist *in vivo* to be more accurately predicted. Second, the changes in architecture during scaffold degradation, such as porosity, pore size and tortuosity, may be successfully measured using this technique.[31] Third, since the technique is already primarily used to investigate the behaviour of cells, the effect that these cells have on scaffold architecture and vice versa may also be examined.

Confocal microscopy may also be used to measure pore strut alignment and orientation, although such methods are only implemented by the occasional study.[57] However, there are numerous accounts of the use of confocal microscopy to measure the orientation of cells or of newly formed tissue within a scaffold,[23,97] and there is no reason why these methods could not also be used to assess the scaffold strut arrangement. This approach is often based on an image analysis technique such as fast Fourier transform.[23,98] The current limitation of this technique, as with so many others, is that there is no standardisation in the quantification of orientation or alignment. The idea of an orientation index to describe scaffold orientation with the use of just one numerical value is promising, but different authors define this in different ways.[6,23] Many authors give only a graphical representation of tissue orientation[103] (an example is given in Fig. 13), but at least this approach is unambiguous in interpretation.

One disadvantage of confocal microscopy is the low penetration depth, or z-extent of the imaging process. Emerging optical techniques may hold the key to this problem. Non-linear optical microscopy, or multiphoton microscopy, is a field of research based on the fact that more than one photon interacting within a molecule in a short time period gives a power law increase in the

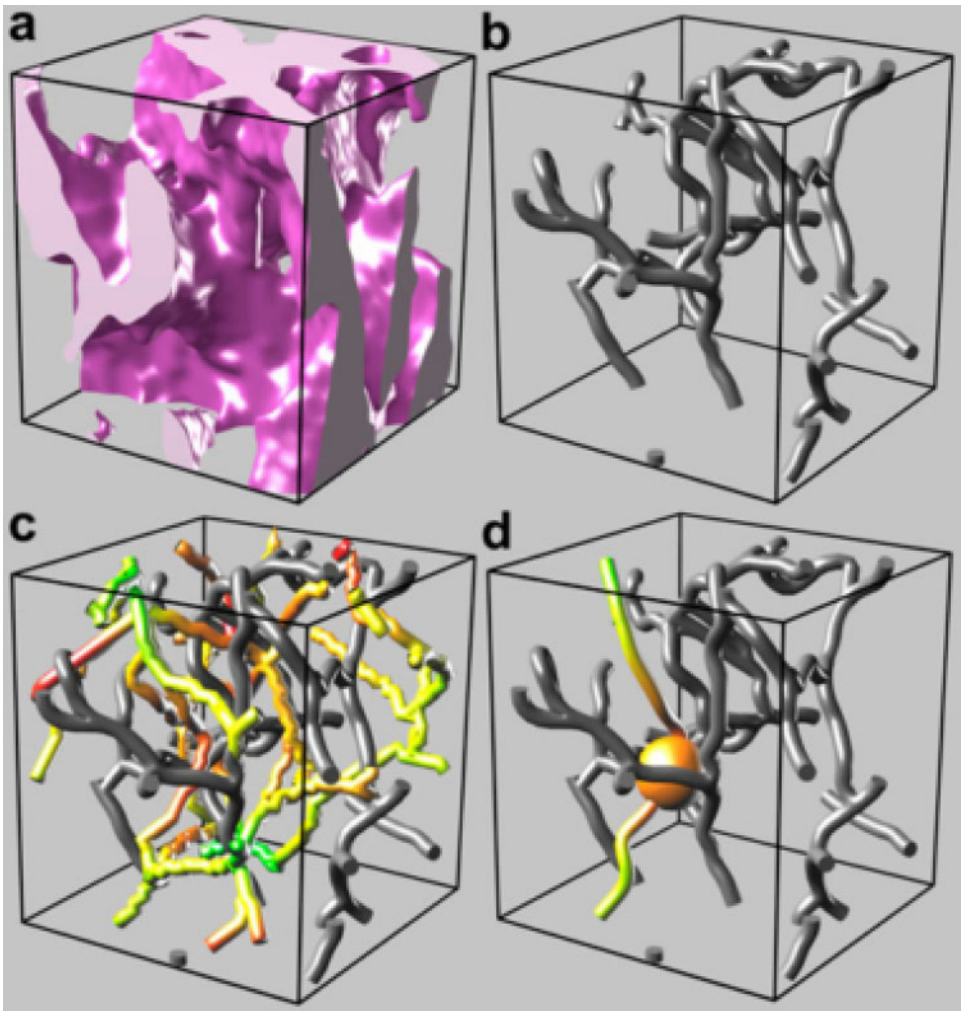

a segmented solid phase; *b* skeletonised solid phase; *c* skeletonised pore space; *d* percolating path of pore space voxels

12 Processing of tomographic dataset obtained using confocal microscopy (reprinted from Ref. 82 with permission from Elsevier)

available signal.[50] The resulting high photon density in the focal volume gives an intrinsic pinhole effect, making the technique analogous to confocal microscopy. Figure 14 gives some examples of images obtained using this technique. The key advantage is that depths >100 μm can be observed.[104] This opens up the possibility of multiphoton microscopy as a future technique for obtaining 3D image datasets of tissue engineering scaffolds in the hydrated state, with the additional option of imaging during dynamic processes such as degradation, cell seeding and even new tissue formation.[99,102] This must be a long term goal, however, due to the current lack of availability and high cost of such systems.

Requirements for future

At the start of this report, four key areas of architectural characterisation were identified, in which tissue engineering research is limited by a lack of standardisation. It has now been demonstrated that the solutions to many of these problems already exist: the issue now is making them more mainstream.

The wide variety of available measurement techniques is not necessarily a problem, so long as it is always acknowledged exactly what characteristic is being defined. In terms of pore size measurement, image analysis will tend to measure the macropore diameter: whether this is measured from an SEM image, a confocal image or a slice from a micro-CT dataset. On the other hand, indirect measurements such as capillary flow porometry will instead measure the constrictions to fluid flow. It is suggested that both approaches are equally valid, but emphasised that they are not interchangeable. A thorough characterisation of a scaffold will include both image analysis and physical pore size measurements.

This dual approach also allows measurement of other parameters simultaneously. From a physical measurement, it is possible to measure permeability. From a 3D tomography dataset, it is possible to measure the interconnectivity characteristics of the scaffold, such as percolation diameter. Currently, the best choice for tomography is micro-CT, but as multiphoton microscopy becomes more widely available, it is hoped that this technique will develop into a more flexible alternative, in order to allow dynamic architectural measurements to be taken.

Conclusions

The link between scaffold architecture and cell response is still far from being completely understood. However, by standardisation of architectural characterisation, a

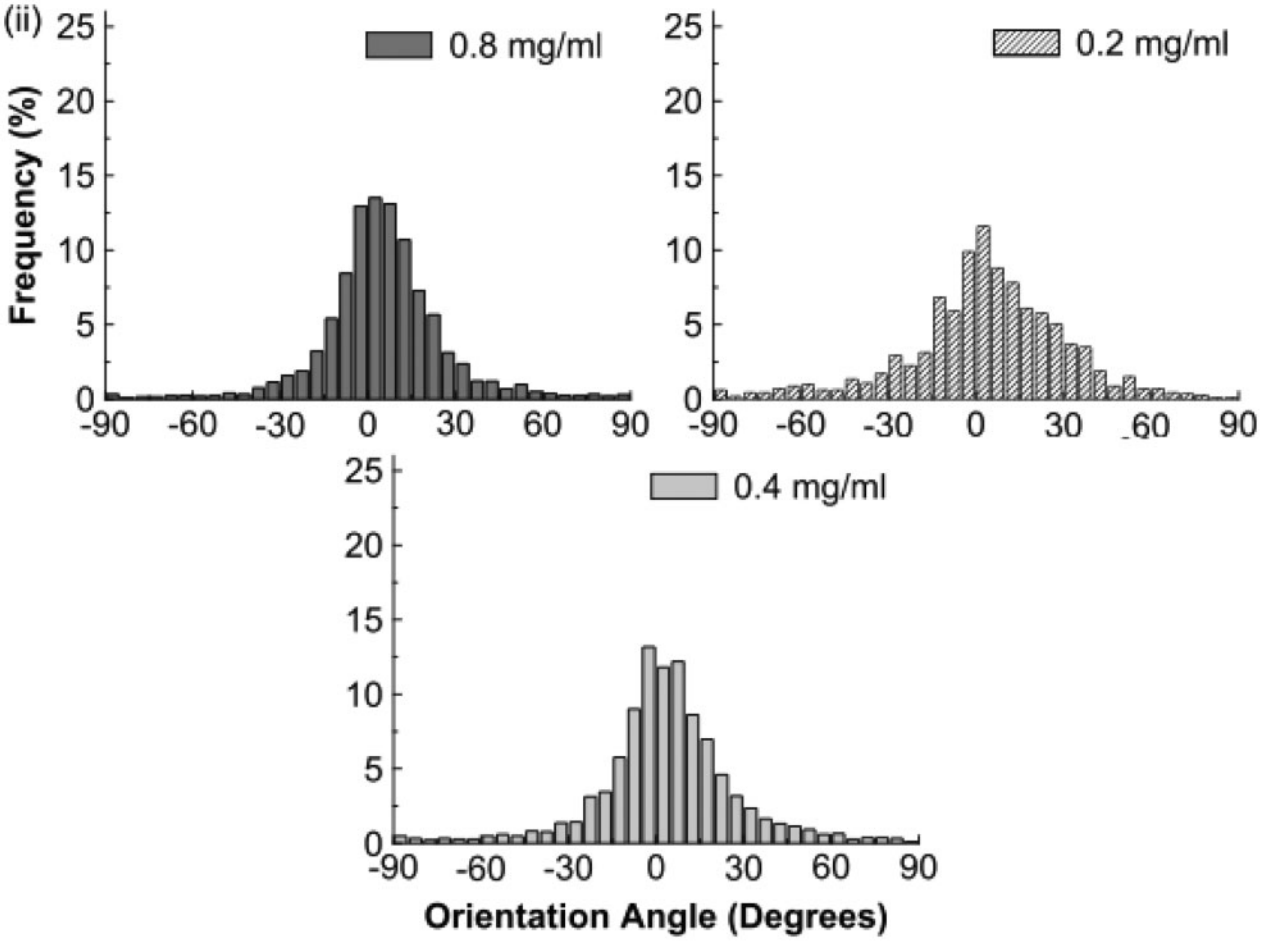

13 Typical approach to displaying fibre orientation in literature: in this case, angle from direction of shear flow deposition is displayed, shown for three different starting concentrations of polymer solution (reprinted from Ref. 103 with permission from Elsevier)

more thorough understanding of how to influence cell behaviour can certainly be achieved. There are various steps that should now be taken in pursuit of this goal:

1. the development of better awareness of the link between measurement technique, measured properties and their scalability
2. emphasis on the combination of indirect (physical) and direct (image-based) measurement techniques
3. further research into the most promising future techniques for 3D image acquisition, such as multiphoton microscopy, allowing better characterisation of scaffold responses to dynamic conditions.

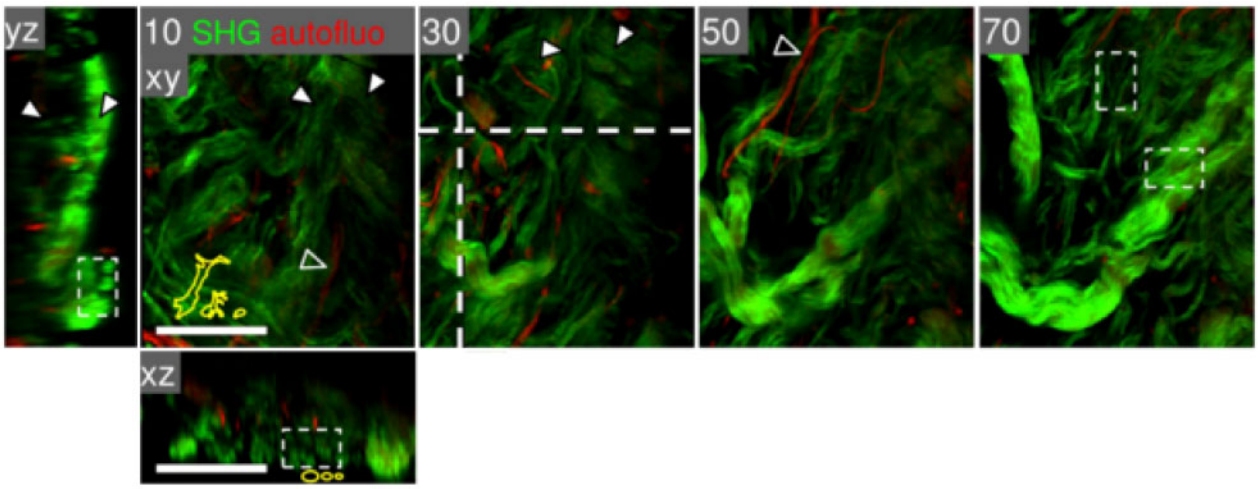

14 Scaffold images obtained using multiphoton microscopy, shown in various sections and at various imaging depths (in um) as indicated at top left of each image. Scale bar 100 um (reprinted from Ref. 104 with permission from Elsevier)

If the above conditions are satisfied, then the ability to identify the ideal scaffold architecture for any desired biological application becomes a realistic prospect.

Acknowledgements

J. Ashworth would like to acknowledge the support of the EPSRC and Geistlich Pharma AG for the provision of PhD funding.

Reference

1. T. M. Freyman and I. V. Yannas: 'Cellular materials as porous scaffolds for tissue engineering', *Prog. Mater. Sci.*, 2001, **46**, (3–4), 273–282.
2. I. V. Yannas, E. Lee, D. P. Orgill, E. M. Skrabut and G. F. Murphy: 'Synthesis and characterization of a model extracellular matrix that induces partial regeneration of adult mammalian skin', *Proc. Natl Acad. Sci. U.S.A*, 1989, **86**, (3), 933–937.
3. S. C. Owen and M. S. Shoichet: 'Design of three-dimensional biomimetic scaffolds', *J. Biomed. Mater. Res. A*, 2010, **94A**, (4), 1321–1331.
4. L. J. Gibson and M. F. Ashby: 'Cellular solids: structure and properties', 1st edn, Chap. 2, 'The structure of cellular solids', Oxford, UK, 11–41; 1988, Pergamon Press.
5. 'Standard guide for interpreting images of polymeric tissue scaffolds', F2603-06, ASTM, West Conshohocken, PA, USA, 2012.
6. M. Madaghiele, A. Sannino, I. V. Yannas and M. Spector: 'Collagen-based matrices with axially oriented pores', *J. Biomed. Mater. Res. A*, 2008, **85A**, (3), 757–767.
7. T. M. Freyman, I. V. Yannas, R. Yokoo and L. J. Gibson: 'Fibroblast contraction of a collagen-GAG matrix', *Biomaterials*, 2001, **22**, (21), 2883–2891.
8. F. J. O'Brien, B. A. Harley, I. V. Yannas and L. Gibson: 'Influence of freezing rate on pore structure in freeze-dried collagen-GAG scaffolds', *Biomaterials*, 2004, **25**, (6), 1077–1086.
9. S. Hofmann, H. Hagenmüller, A. M. Koch, R. Müller, G. Vunjak-Novakovic, D. L. Kaplan, H. P. Merkle and L. Meinel: 'Control of in vitro tissue-engineered bone-like structures using human mesenchymal stem cells and porous silk scaffolds', *Biomaterials*, 2007, **28**, (6), 1152–1162.
10. C. M. Murphy, M. G. Haugh and F. J. O'Brien: 'The effect of mean pore size on cell attachment, proliferation and migration in collagen-glycosaminoglycan scaffolds for bone tissue engineering', *Biomaterials*, 2010, **31**, (3), 461–466.
11. F. J. O'Brien, B. A. Harley, I. V. Yannas and L. J. Gibson: 'The effect of pore size on cell adhesion in collagen-GAG scaffolds', *Biomaterials*, 2005, **26**, (4), 433–441.
12. S. Li, J. R. De Wijn, J. Li, P. Layrolle and K. De Groot: 'Macroporous biphasic calcium phosphate scaffold with high permeability/porosity ratio', *Tissue Eng.*, 2003, **9**, (3), 535–548.
13. J. R. Jones, G. Poologasundarampillai, R. C. Atwood, D. Bernard and P. D. Lee: 'Non-destructive quantitative 3D analysis for the optimisation of tissue scaffolds', *Biomaterials*, 2007, **28**, (7), 1404–1413.
14. P. Tayalia, C. R. Mendonca, T. Baldacchini, D. J. Mooney and E. Mazur: '3D Cell-migration studies using two-photon engineered polymer scaffolds', *Adv. Mater.*, 2008, **20**, (23), 4494–4498.
15. C. M. Murphy, F. J. O'Brien, D. G. Little and A. Schindeler: 'Cell-scaffold interactions in the bone tissue engineering triad', *Eur. Cell. Mater.*, 2013, **26**, 120–132.
16. I. V. Yannas: 'Emerging rules for inducing organ regeneration', *Biomaterials*, 2012, **34**, 321–330.
17. S. T. Ho and D. W. Hutmacher: 'A comparison of micro CT with other techniques used in the characterization of scaffolds', *Biomaterials*, 2006, **27**, (8), 1362–76.
18. S. J. Hollister: 'Porous scaffold design for tissue engineering', *Nat. Mater.*, 2005, **4**, (7), 518–524.
19. S. Y. Lee, B. R. Lee, J. Lee, S. Kim, J. K. Kim, Y. H. Jeong and S. Jin: 'Microscale diffusion measurements and simulation of a scaffold with a permeable strut', *Int. J. Mol. Sci.*, 2013, **14**, (10), 20157–20170.
20. C. M. Tierney, M. G. Haugh, J. Liedl, F. Mulcahy, B. Hayes and F. J. O'Brien: 'The effects of collagen concentration and crosslink density on the biological, structural and mechanical properties of collagen-GAG scaffolds for bone tissue engineering', *J. Mech. Behav. Biomed. Mater.*, 2009, **2**, (2), 202–209.
21. P. Swider, M. Conroy, A. Pédrono, D. Ambard, S. Mantell, K. Søballe and J. E. Bechtold: 'Use of high-resolution MRI for investigation of fluid flow and global permeability in a material with interconnected porosity', *J. Biomech.*, 2007, **40**, (9), 2112–2118.
22. A. Tamayol and M. Bahrami: 'Transverse permeability of fibrous porous media', *Phys. Rev. E*, 2011, **83E**, (4), 046314.
23. G. C. Engelmayr, M. Cheng, C. J. Bettinger, J. T. Borenstein, R. Langer and L. E. Freed: 'Accordion-like honeycombs for tissue engineering of cardiac anisotropy', *Nat. Mater.*, 2008, **7**, (12), 1003–1010.
24. A. Pathak and S. Kumar: 'Biophysical regulation of tumor cell invasion: moving beyond matrix stiffness', *Integr. Biol.*, 2011, **3**, (4), 267–278.
25. J. F. Mano, G. A. Silva, H. S. Azevedo, P. B. Malafaya, R. A. Sousa, S. S. Silva, L. F. Boesel, J. M. Oliveira, T. C. Santos, A. P. Marques, N. M. Neves and R. L. Reis: 'Natural origin biodegradable systems in tissue engineering and regenerative medicine: present status and some moving trends', *J. R. Soc. Interface*, 2007, **4**, (17), 999–1030.
26. T. Hayashi: 'Biodegradable polymers for biomedical uses', *Prog. Polym. Sci.*, 1994, **19**, 663–702.
27. V. Y. Chakrapani and A. Gnanamani: 'Electrospinning of type I collagen and PCL nanofibers using acetic acid', *J. Appl. Polym. Sci.*, 2012, **125**, (4), 3221–3227.
28. C. Liu, Z. Xia and J. T. Czernuszka: 'Design and development of three-dimensional scaffolds for tissue engineering', *Chem. Eng. Res. Des.*, 2007, **85**, (7), 1051–1064.
29. S. Deville, E. Saiz and A. P. Tomsia: 'Freeze casting of hydroxyapatite scaffolds for bone tissue engineering', *Biomaterials*, 2006, **27**, (32), 5480–5489.
30. B. Inanc, A. E. Elcin and Y. M. Elcin: 'Osteogenic induction of human periodontal ligament fibroblasts under two-and three-dimensional culture conditions', *Tissue Eng.*, 2006, **12**, (2), 257–266.
31. J. S. Tjia and P. V. Moghe: 'Analysis of 3-D microstructure of porous poly(lactide-glycolide) matrices using confocal microscopy', *J. Biomed. Mater. Res. A*, 1998, **43A**, (3), 291–299.
32. S. Sell, C. Barnes, D. Simpson and G. Bowlin: 'Scaffold permeability as a means to determine fiber diameter and pore size of electrospun fibrinogen', *J. Biomed. Mater. Res. A*, 2008, **85A**, (1), 115–126.
33. K. M. Pawelec, A. Husmann, S. M. Best and R. E. Cameron: 'A design protocol for tailoring ice-templated scaffold structure', *J. R. Soc. Interface*, 2014, **11**, (92), 20130958.
34. H. Schoof, L. Bruns, A. Fischer, I. Heschel and G. Rau: 'Dendritic ice morphology in unidirectionally solidified collagen suspensions', *J. Cryst. Growth*, 2000, **209**, (1), 122–129.
35. A. G. Mitsak and J. M. Kemppainen: 'Effect of polycaprolactone scaffold permeability on bone regeneration in vivo', *Tissue Eng. A*, 2011, **17A**, (13–14), 1831–1839.
36. M. de Barros Coelho and M. Magalhães Pereira: 'Sol–gel synthesis of bioactive glass scaffolds for tissue engineering: effect of surfactant type and concentration', *J. Biomed. Mater. Res. B*, 2005, **75B**, (2), 451–456.
37. 'Standard guide for assessing microstructure of polymeric scaffolds for use in tissue-engineered medical products', F2450-10, ASTM, West Conshohocken, PA, USA, 2010.
38. M. Gelinsky, P. B. Welzel, P. Simon, A. Bernhardt and U. König: 'Porous three-dimensional scaffolds made of mineralised collagen: Preparation and properties of a biomimetic nanocomposite material for tissue engineering of bone', *Chem. Eng. J.*, 2008, **137**, (1), 84–96.
39. A. Jena and K. Gupta: 'Characterization of pore structure of filtration media', *Fluid/Particle Sep. J.*, 2002, **4**, (3), 227–241.
40. K. Whang, C. H. Thomas, K. E. Healy and G. Nuber: 'A novel method to fabricate bioabsorbable scaffolds', *Polymer (Guildf).*, 1995, **36**, (4), 837–842.
41. S.-N. Park, J.-C. Park, H. O. Kim, M. J. Song and H. Suh: 'Characterization of porous collagen/hyaluronic acid scaffold modified by 1-ethyl-3-(3-dimethylaminopropyl)carbodiimide cross-linking', *Biomaterials*, 2002, **23**, (4), 1205–1212.
42. L. Buttafoco, P. Engbers-Buijtenhuijs, A. A. Poot, P. J. Dijkstra, W. F. Daamen, T. H. van Kuppevelt, I. Vermes and J. Feijen: 'First steps towards tissue engineering of small-diameter blood vessels: preparation of flat scaffolds of collagen and elastin by means of freeze drying', *J. Biomed. Mater. Res. B*, 2006, **77B**, (2), 357–68.

43. 'Standard test method for stereological evaluation of porous coatings on medical implants', F1854-09, ASTM, West Conshohocken, PA, USA, 2009.
44. M. G. Haugh, C. M. Murphy and F. J. O'Brien: 'Novel freeze-drying methods to produce a range of collagen-glycosaminoglycan scaffolds with tailored mean pore sizes', *Tissue Eng. C*, 2010, **16C**, (5), 887–894.
45. N. Davidenko, T. Gibb, C. Schuster, S. M. Best, J. J. Campbell, C. J. Watson and R. E. Cameron: 'Biomimetic collagen scaffolds with anisotropic pore architecture', *Acta Biomater.*, 2012, **8**, (2), 667–676.
46. K. M. Pawelec, A. Husmann, S. M. Best and R. E. Cameron: 'Understanding anisotropy and architecture in ice-templated biopolymer scaffolds', *Mater. Sci. Eng. C*, 2014, **C37**, 141–147.
47. G. Incera Garrido, F. C. Patcas, S. Lang and B. Kraushaar-Czarnetzki: 'Mass transfer and pressure drop in ceramic foams: a description for different pore sizes and porosities', *Chem. Eng. Sci.*, 2008, **63**, (21), 5202–5217.
48. R. C. Atwood, J. R. Jones, P. D. Lee and L. L. Hench: 'Analysis of pore interconnectivity in bioactive glass foams using X-ray microtomography', *Scr. Mater.*, 2004, **51**, (11), 1029–1033.
49. A. C. Jones, C. H. Arns, D. W. Hutmacher, B. K. Milthorpe, A. P. Sheppard and M. A. Knackstedt: 'The correlation of pore morphology, interconnectivity and physical properties of 3D ceramic scaffolds with bone ingrowth', *Biomaterials*, 2009, **30**, (7), 1440–1451.
50. M. Vielreicher, S. Schürmann, R. Detsch, M. A. Schmidt, A. Buttgereit, A. Boccaccini and O. Friedrich: 'Taking a deep look: modern microscopy technologies to optimize the design and functionality of biocompatible scaffolds for tissue engineering in regenerative medicine', *J. R. Soc. Interface*, 2013, **10**, (86), 20130263.
51. T. L. Kline and E. L. Ritman: 'Characterization of the pore labyrinth geometry of sea sponges imaged by micro-CT', *J. Porous Mater.*, 2012, **19**, (2), 141–151.
52. M. J. Moore, E. Jabbari, E. L. Ritman, L. Lu, B. L. Currier, A. J. Windebank and M. J. Yaszemski: 'Quantitative analysis of interconnectivity of porous biodegradable scaffolds with micro-computed tomography', *J. Biomed. Mater. Res. A*, 2004, **71A**, (2), 258–267.
53. B. Otsuki, M. Takemoto, S. Fujibayashi, M. Neo, T. Kokubo and T. Nakamura: 'Pore throat size and connectivity determine bone and tissue ingrowth into porous implants: three-dimensional micro-CT based structural analyses of porous bioactive titanium implants', *Biomaterials*, 2006, **27**, (35), 5892–5900.
54. G. Fostad, B. Hafell, A. Førde, R. Dittmann, R. Sabetrasekh, J. Will, J. E. Ellingsen, S. P. Lyngstadaas and H. J. Haugen: 'Loadable TiO_2 scaffolds – a correlation study between processing parameters, micro CT analysis and mechanical strength', *J. Eur. Ceram. Soc.*, 2009, **29**, (13), 2773–2781.
55. F. J. O'Brien, B. A. Harley, M. A. Waller, I. V. Yannas, L. J. Gibson and P. J. Prendergast: 'The effect of pore size on permeability and cell attachment in collagen scaffolds for tissue engineering', *Technol. Health Care*, 2007, **15**, (1), 3–17.
56. M. Galli, E. Fornasiere, J. Cugnoni and M. L. Oyen: 'Poroviscoelastic characterization of particle-reinforced gelatin gels using indentation and homogenization', *J. Mech. Behav. Biomed. Mater.*, 2011, **4**, (4), 610–617.
57. S. R. Caliari and B. A. C. Harley: 'The effect of anisotropic collagen-GAG scaffolds and growth factor supplementation on tendon cell recruitment, alignment, and metabolic activity', *Biomaterials*, 2011, **32**, (23), 5330–5340.
58. H. Schoof, J. Apel, I. Heschel and G. Rau: 'Control of pore structure and size in freeze-dried collagen sponges', *J. Biomed. Mater. Res.*, 2001, **58**, (4), 352–357.
59. S. I. Jeong, S. Y. Kim, S. K. Cho, M. S. Chong, K. S. Kim, H. Kim, S. B. Lee and Y. M. Lee: 'Tissue-engineered vascular grafts composed of marine collagen and PLGA fibers using pulsatile perfusion bioreactors', *Biomaterials*, 2007, **28**, (6), 1115–1122.
60. A. S. P. Lin, T. H. Barrows, S. H. Cartmell and R. E. Guldberg: 'Microarchitectural and mechanical characterization of oriented porous polymer scaffolds', *Biomaterials*, 2003, **24**, (3), 481–489.
61. M. Hacker, M. Ringhofer, B. Appel, M. Neubauer, T. Vogel, S. Young, A. G. Mikos, T. Blunk, A. Göpferich and M. B. Schulz: 'Solid lipid templating of macroporous tissue engineering scaffolds', *Biomaterials*, 2007, **28**, (24), 3497–3507.
62. H. Mehdizadeh, S. Sumo, E. S. Bayrak, E. M. Brey and A. Cinar: 'Three-dimensional modeling of angiogenesis in porous biomaterial scaffolds', *Biomaterials*, 2013, **34**, (12), 2875–2887.
63. Y.-G. Ko, N. Kawazoe and T. Tateishi: 'Preparation of novel collagen sponges using an ice particulate template', *J. Bioact. Compat. Polym.*, 2010, **25**, (4), 360–373.
64. B. B. Mandal and S. C. Kundu: 'Cell proliferation and migration in silk fibroin 3D scaffolds', *Biomaterials*, 2009, **30**, (15), 2956–2965.
65. F. A. Maspero, K. Ruffieux, B. Müller and E. Wintermantel: 'Resorbable defect analog PLGA scaffolds using CO_2 as solvent: structural characterization', *J. Biomed. Mater. Res.*, 2002, **62**, (1), 89–98.
66. G. Lemon, Y. Reinwald, L. J. White, S. M. Howdle, K. M. Shakesheff and J. R. King: 'Interconnectivity analysis of supercritical CO_2-foamed scaffolds', *Comput. Methods Programs Biomed.*, 2012, **106**, (3), 139–149.
67. B. A. C. Harley, H.-D. Kim, M. H. Zaman, I. V. Yannas, D. A. Lauffenburger and L. J. Gibson: 'Microarchitecture of three-dimensional scaffolds influences cell migration behavior via junction interactions', *Biophys. J.*, 2008, **95**, (8), 4013–4024.
68. A. G. Evans, J. W. Hutchinson and M. F. Ashby: 'Multifunctionality of cellular metal systems', *Prog. Mater. Sci.*, 1999, **43**, 171–221.
69. J. Banhart: 'Manufacture, characterisation and application of cellular metals and metal foams', *Prog. Mater. Sci.*, 2001, **46**, (6), 559–632.
70. L. L. Hench and J. M. Polak: 'Third-generation biomedical materials', *Science*, 2002, **295**, (5557), 1014–1017.
71. D. J. Green and P. Colombo: 'Cellular ceramics: intriguing structures, novel properties, and innovative applications', *MRS Bull.*, 2003, **28**, (4), 296–300.
72. C. L. Lin and J. D. Miller: 'Network analysis of filter cake pore structure by high resolution X-ray microtomography', *Chem. Eng. J.*, 2000, **77**, 272–280.
73. R. Bagherzadeh, M. Latifi, S. S. Najar, M. A. Tehran and L. Kong: 'Three-dimensional pore structure analysis of nano/microfibrous scaffolds using confocal laser scanning microscopy', *J. Biomed. Mater. Res. A*, 2013, **101A**, (3), 765–774.
74. P. Levitz: 'Toolbox for 3D imaging and modeling of porous media: relationship with transport properties', *Cem. Concr. Res.*, 2007, **37**, (3), 351–359.
75. M. A. B. Promentilla, T. Sugiyama, T. Hitomi and N. Takeda: 'Quantification of tortuosity in hardened cement pastes using synchrotron-based X-ray computed microtomography', *Cem. Concr. Res.*, 2009, **39**, (6), 548–557.
76. B. Starly, E. Yildirim and W. Sun: 'A tracer metric numerical model for predicting tortuosity factors in three-dimensional porous tissue scaffolds', *Comput. Methods Programs Biomed.*, 2007, **87**, (1), 21–27.
77. Y. Nakashima and T. Yamaguchi: 'DMAP.m: A Mathematica® program for three-dimensional mapping of tortuosity and porosity of porous media', *Bull. Geol. Soc. Jpn*, 2004, **55**, (3/4), 93–103.
78. Y. Bernabé, U. Mok and B. Evans: 'Permeability–porosity relationships in rocks subjected to various evolution processes', *Pure Appl. Geophys.*, 2003, **160**, 937–960.
79. J. Liu, K. Regenauer-Lieb, C. Hines, K. Liu, O. Gaede and A. Squelch: 'Improved estimates of percolation and anisotropic permeability from 3-D X-ray microtomography using stochastic analyses and visualization', *Geochem. Geophys. Geosyst.*, 2009, **10**, (5), 1–13.
80. J. Liu and K. Regenauer-Lieb: 'Application of percolation theory to microtomography of structured media: percolation threshold, critical exponents, and upscaling', *Phys. Rev. E*, 2011, **83E**, (1), 016106.
81. P. Sotta and D. Long: 'The crossover from 2D to 3D percolation: theory and numerical simulations', *Eur. Phys. J. E*, 2003, **11E**, (4), 375–387.
82. W. Mickel, S. Münster, L. M. Jawerth, D. A. Vader, D. A. Weitz, A. P. Sheppard, K. Mecke, B. Fabry and G. E. Schröder-Turk: 'Robust pore size analysis of filamentous networks from three-dimensional confocal microscopy', *Biophys. J.*, 2008, **95**, (12), 6072–6080.
83. Z. Zhou, J. Yang, R. M. Ziff and Y. Deng: 'Crossover from isotropic to directed percolation', *Phys. Rev. E*, 2012, **1E**, (86), 1–8.
84. M. J. Saxton: 'Two-dimensional continuum percolation threshold for diffusing particles of nonzero radius', *Biophys. J.*, 2010, **99**, (5), 1490–1499.
85. E. Maire and P. J. Withers: 'Quantitative X-ray tomography', *Int. Mater. Rev.*, 2014, **59**, (1), 1–43.

86. J. T. Fredrich: '3D imaging of porous media using laser scanning confocal microscopy with application to microscale transport processes', *Phys. Chem. Earth A*, 1999, **24**, (7), 551–561.
87. I. Balberg: 'Recent developments in continuum percolation', *Philos. Mag. B*, 1987, **56B**, (6), 991–1003.
88. G. P. Raeber, M. P. Lutolf and J. A. Hubbell: 'Molecularly engineered PEG hydrogels: a novel model system for proteolytically mediated cell migration', *Biophys. J.*, 2005, **89**, (2), 1374–1388.
89. L. Wu and J. Ding: 'In vitro degradation of three-dimensional porous poly(D,L-lactide-co-glycolide) scaffolds for tissue engineering', *Biomaterials*, 2004, **25**, (27), 5821–5830.
90. E. C. Soller, D. S. Tzeranis, K. Miu, P. T. C. So and I. V. Yannas: 'Common features of optimal collagen scaffolds that disrupt wound contraction and enhance regeneration both in peripheral nerves and in skin', *Biomaterials*, 2012, **33**, (19), 4783–4791.
91. D. Dado and S. Levenberg: 'Cell-scaffold mechanical interplay within engineered tissue', *Semin. Cell Dev. Biol.*, 2009, **20**, (6), 656–664.
92. G. Kerckhofs and J. Schrooten: 'Mechanical characterization of porous structures by the combined use of micro-CT and in-situ loading', Proc. 17th World Conf. on 'Nondestructive testing', Shanghai, China, October 2008, Chinese Society for Nondestructive Testing, 47.
93. M. Stauber and R. Müller: 'Micro-computed tomography: a method for the non-destructive evaluation of the three-dimensional structure of biological specimens', in 'Osteoporosis: methods molecular biology', Totowa, NJ, USA, (ed. J. J. Westendorf), 273–291; 2008, Humana Press.
94. C. N. Grover, R. E. Cameron and S. M. Best: 'Investigating the morphological, mechanical and degradation properties of scaffolds comprising collagen, gelatin and elastin for use in soft tissue engineering', *J. Mech. Behav. Biomed. Mater.*, 2012, **10**, 62–74.
95. N. Davidenko, J. J. Campbell, E. S. Thian, C. J. Watson and R. E. Cameron: 'Collagen-hyaluronic acid scaffolds for adipose tissue engineering', *Acta Biomater.*, 2010, **6**, (10), 3957–68.
96. A. M. Donald: 'The use of environmental scanning electron microscopy for imaging wet and insulating materials', *Nat. Mater.*, 2003, **2**, (8), 511–516.
97. G. C. Engelmayr, G. D. Papworth, S. C. Watkins, J. E. Mayer and M. S. Sacks: 'Guidance of engineered tissue collagen orientation by large-scale scaffold microstructures', *J. Biomech.*, 2006, **39**, (10), 1819–1831.
98. N. F. Huang, J. Okogbaa, J. C. Lee, A. Jha, T. S. Zaitseva, M. V. Paukshto, J. S. Sun, N. Punjya, G. G. Fuller and J. P. Cooke: 'The modulation of endothelial cell morphology, function, and survival using anisotropic nanofibrillar collagen scaffolds', *Biomaterials*, 2013, **34**, (16), 4038–4047.
99. W.-L. Chen, C.-H. Huang, L.-L. Chiou, T.-H. Chen, Y.-Y. Huang, C.-C. Jiang, H.-S. Lee and C.-Y. Dong: 'Multiphoton imaging and quantitative analysis of collagen production by chondrogenic human mesenchymal stem cells cultured in chitosan scaffold', *Tissue Eng. C*, 2010, **16C**, (5), 913–920.
100. S. Chuayjuljit, A. Maungchareon and O. Saravari: 'Preparation and properties of palm oil-based rigid polyurethane nanocomposite foams', *J. Reinf. Plast. Compos.*, 2010, **29**, (2), 218–225.
101. J. Grosse, B. Dietrich, G. I. Garrido, P. Habisreuther, N. Zarzalis, H. Martin, M. Kind and B. Kraushaar-Czarnetzki: 'Morphological characterization of ceramic sponges for applications in chemical engineering', *Ind. Eng. Chem. Res.*, 2009, **48**, (23), 10395–10401.
102. M. C. Sukop and G. J. Van Dijk: 'Percolation thresholds in 2-dimensional prefractal models of porous media', *Transp. Porous Media*, 2002, **48**, 187–208.
103. B. Lanfer, U. Freudenberg, R. Zimmermann, D. Stamov, V. Körber and C. Werner: 'Aligned fibrillar collagen matrices obtained by shear flow deposition', *Biomaterials*, 2008, **29**, (28), 3888–3895.
104. K. Wolf, S. Alexander, V. Schacht, L. M. Coussens, U. H. von Andrian, J. van Rheenen, E. Deryugina and P. Friedl: 'Collagen-based cell migration models in vitro and in vivo', *Semin. Cell Dev. Biol.*, 2009, **20**, (8), 931–941.